DOI: 10.1002/ejic.200801104

Late Transition-Metal Complexes of 2-$Ph_2PC_6H_4NHC(O)CH_2NHCO_2Bz$: Observation of Three Distinct Ligation Modes (κ^1-P,κ^2-P/N and κ^3-P/N/N′)

Mark R. J. Elsegood,[a] Andrew J. Lake,[a] and Martin B. Smith*[a]

Keywords: Coordination modes / Metallacycles / P ligands / Late-transition metals

The one-step synthesis of the amide-functionalised tertiary phosphane 2-$Ph_2PC_6H_4NHC(O)CH_2NHCO_2Bz$ (Bz = CH_2Ph), **2·HH**, by condensation of the known aminophosphane, 2-$Ph_2PC_6H_4(NH_2)$ (**1**), with *N*-(benzyloxycarbonyl)-glycine and dicyclohexylcarbodiimide (DCC) in THF at room temperature is reported. The new ligand **2·HH** displays various coordination modes when complexed to a range of late transition-metal precursors. Hence κ^1-P-coordination for **2·HH** is observed in the complexes ClAu(**2·HH**) (**3**), $MCl_2(\eta^5$-$Cp^*)$(**2·HH**) (M = Rh **4**; Ir **5**), $RuCl_2(\eta^6$-*p*-cymene)(**2·HH**) (**6**), Pd(κ^2-CN-$C_{12}H_{12}N$)Cl(**2·HH**) (**7**) and MCl_2(**2·HH**)$_2$ (M = Pd **8**; Pt **9**). Treatment of **8** or **9** with *t*BuOK in CH_3OH gave the bis-κ^2-P/N-chelate complexes *cis*-M{2-$Ph_2PC_6H_4NC(O)CH_2$-$NHCO_2Bz$}$_2$ (M = Pt **10**; Pd **11**) in which both monoanionic ligands **2·H**$^-$ are disposed in a *cis* geometry. The related nickel(II) complex *cis*-Ni{2-$Ph_2PC_6H_4NC(O)CH_2NHCO_2$-Bz}$_2$ (**12**) was prepared from $NiCl_2{\cdot}6H_2O$, 2 equiv. of **2·HH** and *t*BuOK in refluxing CH_3OH. Reaction of the piano-stool complex **5** with *t*BuOK in CH_3OH gave the chiral-at-metal complex Ir(η^5-Cp^*){2-$Ph_2PC_6H_4NC(O)CH_2NCO_2Bz$} (**14**), present in solution as two diastereomers. A single-crystal X-ray diffraction study of **14** confirmed the κ^3-P/N/N′-tridentate coordination mode. Under similar conditions the chiral-at-metal ruthenium(II) complex Ru(η^6-*p*-cymene){2-$Ph_2PC_6H_4NC(O)CH_2NCO_2Bz$} (**15**) was prepared in which **2**$^{2-}$ functions efficiently as a dianionic tridentate ligand. All new compounds have been characterised by multinuclear NMR [$^{31}P\{^1H\}$, ^1H], FT-IR, EI-MS, ES-MS and microanalysis. Furthermore, the X-ray structures of ten compounds have been determined and reveal, in the majority of cases, a strong propensity for the –$NHC(O)CH_2NHCO_2Bz$ group to engage in N–H···N, N–H···O and N–H···Cl hydrogen bonding.

Introduction

Coordination compounds of tridentate and tetradentate ligands continue to attract much interest for their variable ligating capabilities,[1–3] stabilisation of G-quadruplex DNA,[4] sensor,[5] magnetic[6] and luminescent[7–9] properties and catalytic applications.[10] Various donor atom combinations have been documented that contain at least one phosphorus donor atom and include for example P/N/C,[11] P/C/N,[12] P/N/N,[13] P/N/O,[14] P/N/S,[15] P/N/P[16] and P/N/Se.[17] Pincer ligands based on P/C/P[18] or P/Si/P[19] donor sets afford interesting complexes, display unusual reactivity and find applications in catalysis. Furthermore, P/O/O and P/O/P ligands have been employed in self-assembly reactions.[20,21] More recently the use of one or two soft selenium donor atoms in tridentate ligands of the type Se/N/O and Se/C/Se have been documented.[22,23]

One of the most common methods for the synthesis of potentially tridentate ligand systems usually involves a Schiff base condensation reaction.[24] This method is particularly applicable to P/N/N and P/N/O ligands. Many of these ligands bind to metals in a neutral κ^3-tridentate fashion or ligate in a singly deprotonated form. Examples of κ^3-tridentate ligands that utilise all three donor centres in a doubly deprotonated form are uncommon.[15] Herein, we report the synthesis of an unsymmetrical κ^3-P/N/N′-ligand and demonstrate the flexible ligation behaviour of this new ligand (in its neutral, monoanionic and dianionic forms) through complexation studies towards linear, pseudo-tetrahedral and square-planar transition-metal centres. All compounds have been characterized by multinuclear NMR and FT-IR spectroscopy and in ten cases by single-crystal X-ray diffraction studies.

Results and Discussion

Ligand Synthesis

The new ligand 2-$Ph_2PC_6H_4NHC(O)CH_2NHCO_2Bz$ (Bz = CH_2Ph) (**2·HH**) was synthesised in moderate yield (36%) by condensation of the amine-functionalised tertiary phosphane 2-$Ph_2PC_6H_4(NH_2)$ (**1**) with *N*-(benzyloxycarbonyl)-glycine and DCC in THF (Scheme 1). Purification of the crude material comprising **2·HH** and unreacted **1** was readily accomplished by recrystallisation from CH_2Cl_2/Et_2O.

[a] Department of Chemistry, Loughborough University, Loughborough, Leics, LE11 3TU, UK
Fax: +44-1509-223925
E-mail: m.b.smith@lboro.ac.uk

Supporting information for this article is available on the WWW under http://www.eurjic.org or from the author.

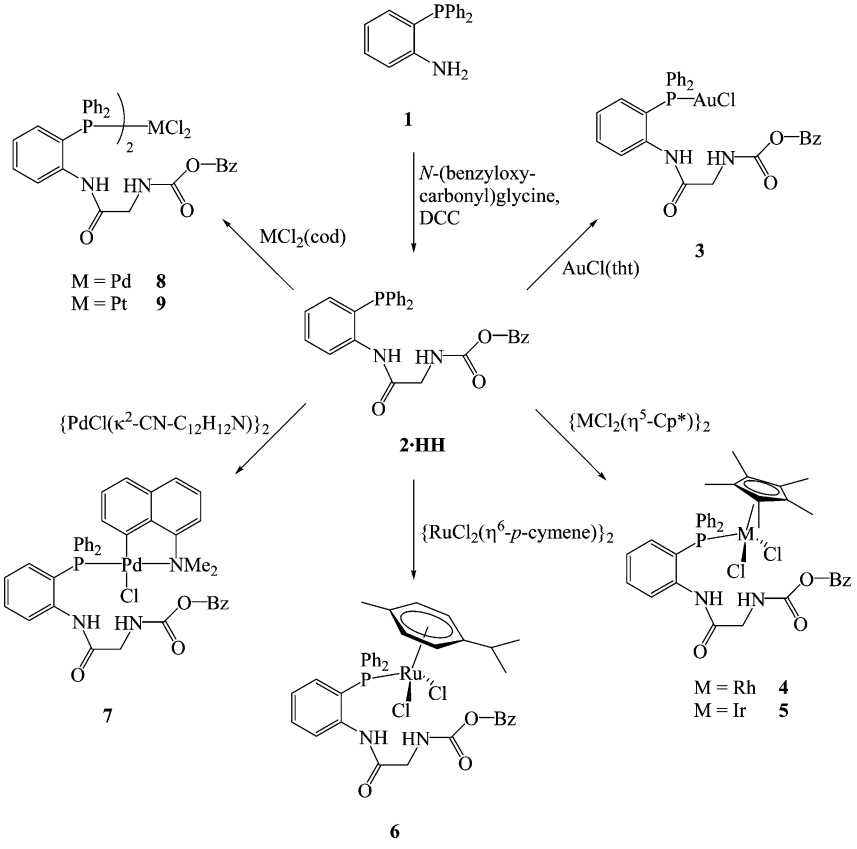

Scheme 1.

The $^{31}P\{^{1}H\}$ NMR spectrum of **2·HH** shows two resonances at δ(P) = –20.7/–21.3 ppm [cf. 2-$Ph_2PC_6H_4(NH_2)$: δ(P) = –20.3 ppm, $CDCl_3$]. The formation of the new C–N bond was further supported by the observation of new resonances at δ(H) = 5.12 (overlapping NH and OCH_2 protons) and a doublet at δ = 3.85 ppm ($NHCH_2$) in the ^1H NMR spectrum. The FT-IR spectrum of **2·HH** clearly shows the presence of NH (3328 and 3264 cm^{-1}) and CO (1721 and 1677 cm^{-1}) functional groups. Oxidation of **2·HH** with aqueous H_2O_2 gives a smooth conversion to the tertiary phosphane oxide **2a** as inferred by two downfield ^{31}P resonances [δ(P) = 37.2 and 36.9 ppm]. The observation of two similar phosphorus signals for **2a** (and **2·HH**), in the region typically expected for tertiary phosphane oxides, suggests closely related structures which we believe to be conformers due to restricted rotation about either the NH–C(O) or NH–C(O)O bonds.

To evaluate whether **2·HH** is preorganised for metal-ion coordination, an X-ray crystallographic study was performed. The molecular structure of **2·HH** (Figure 1) clearly shows that C–N coupling [C(7)–N(1) = 1.417(2) Å, Table 1] has resulted as previously indicated by the spectroscopic data. Pyramidalisation around P(1) is clearly reflected in the C–P–C bond angles which lie in the range 99.11(9)–105.14(9)°. The donor atoms P(1), N(1) and N(2) essentially all reside in the same plane and are positioned towards each other. This finding contrasts with the X-ray crystal structure of 2-{$Ph_2PC_6H_4C(H)=N\}C_6H_4\{NHC(O)CH_2NHCO_2$-Bz}, recently reported by us, in which the -PPh_2 group points away from the N_3 core.[25] The hydrogen H(1) forms an intramolecular hydrogen bond to N(2) [N(1)···N(2) 2.720(2) Å, H(1)···N(2) 2.22(2) Å, N(1)–H(1)···N(2) 116.3(17)°] and H(2) intermolecularly H-bonds to O(1B) [N(2)···O(1B) 2.927(2) Å, H(2)···O(1B) 2.09(2) Å, N(2)–H(2)···O(1B) 162(2)°. Symmetry operator: *B*: *x* + 1/2, *y*, –*z* + 3/2] leading to 1-D chains along the crystallographic *a* direction (Figure 2).

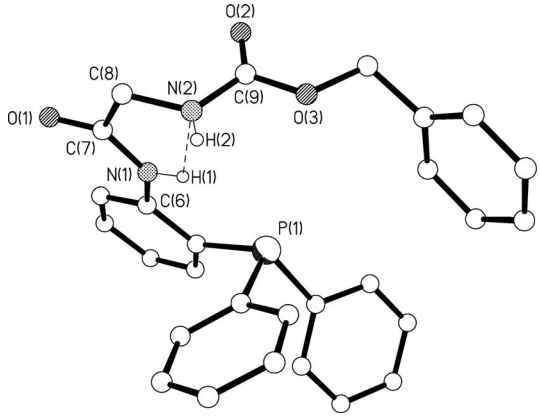

Figure 1. Molecular structure of **2·HH** showing the N(1)–H(1)···N(2) intramolecular H-bonding. All hydrogen atoms except H(1) and H(2) have been omitted for clarity.

Table 1. Selected bond lengths [Å] and angles [°] for compounds **2·HH**, **2a**, **3**, **4**·Et_2O and **8**.

	2·HH	**2a**[a]	**3** (M = Au)	**4**·Et_2O (M = Rh)	**8** (M = Pd)
C(6)–N(1)	1.417(2)	1.408(2) [1.4110(19)]	1.428(4)	1.411(11)	1.418(4)
N(1)–C(7)	1.354(2)	1.357(2) [1.3507(19)]	1.356(5)	1.385(11)	1.344(4)
C(7)–O(1)	1.227(2)	1.2190(19) [1.2234(19)]	1.225(4)	1.221(14)	1.220(4)
N(2)–C(9)	1.355(3)	1.342(2) [1.346(2)]	1.348(5)	1.385(15)	1.326(6)
C(9)–O(2)	1.210(2)	1.216(2) [1.2143(19)]	1.208(5)	1.171(14)	1.209(5)
C(9)–O(3)	1.348(2)	1.355(2) [1.3545(19)]	1.363(5)	1.348(12)	1.367(5)
P(1)–O(7)		1.5023(11) [1.4989(11)]			
M(1)–Cl(1)			2.3111(9)	2.4180(19)	2.2999(8)
M(1)–Cl(2)				2.4086(19)	
M(1)–P(1)			2.2326(9)	2.353(2)	2.3288(8)
M(1)–M(1A)			3.0926(9)		
M(1)–$C_{centroid}$				1.8343(34)	
C(6)–N(1)–C(7)	130.32(17)	128.37(14) [128.59(13)]	123.9(3)	124.9(8)	126.8(3)
N(1)–C(7)–O(1)	125.76(19)	126.02(16) [125.74(15)]	123.7(4)	122.5(10)	124.5(3)
N(2)–C(9)–O(2)	125.15(19)	125.03(16) [125.46(15)]	125.8(4)	123.0(10)	126.2(4)
O(2)–C(9)–O(3)	124.79(19)	124.03(17) [125.22(15)]	124.2(4)	128.9(11)	123.3(4)
P(1)–M(1)–Cl(1)			169.99(3)	93.25(7)	86.12(3)
P(1′)–M(1)–Cl(1)					93.88(3)
P(1)–M(1)–Cl(2)				89.95(7)	
Cl(1)–M(1)–Cl(2)				89.56(8)	
P(1)–M(1)–M(1A)			111.47(3)		
Cl(1)–M(1)–M(1A)			74.70(2)		

[a] Two independent molecules in the asymmetric unit. Symmetry operator: A: $x + 1/2$, y, $-z + 3/2$. Symmetry operator: ′: $-x + 1$, $-y + 1$, $-z + 1$.

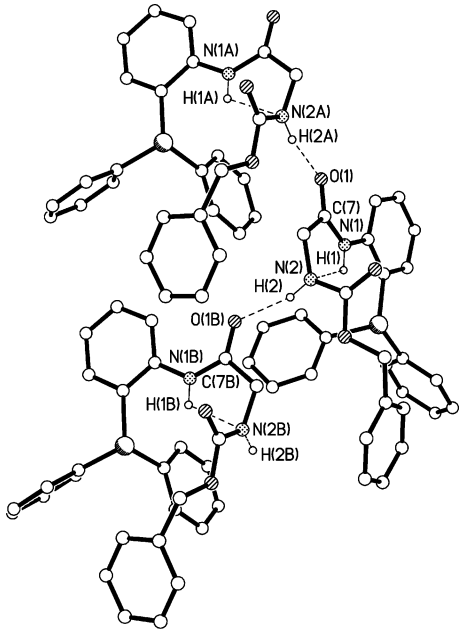

Figure 2. Intermolecular N–H···O bonding in **2·HH**. Symmetry operator: A: $x + 1/2$, y, $-z + 3/2$. Only the N–H hydrogen atoms are shown for clarity.

The structure of the phosphane oxide **2a** (Figure 3) has also been determined with selected bond lengths and angles given in Table 1. Overall the structure is similar to **2·HH** with the exception of the newly formed P=O bond [1.5023(11) Å and 1.4989(11) Å for the two independent molecules]. In contrast with **2·HH**, H(1) [and H(3)] are involved in bifurcated intramolecular H-bonding with the secondary amine nitrogen [N(2) and N(4), respectively] and the phosphoryl oxygen [O(7) and O(8), respectively] atoms [N(1)···N(2)2.743(2) Å,H(1)···N(2)2.280(18) Å,N(1)–H(1)···N(2) 113.9(15)° and N(1)···O(7) 2.7394(17) Å, H(1)···O(7) 1.979(19) Å, N(1)–H(1)···O(7) 146.8(17)°. Equivalent parameters for the second independent molecule are N(3)···N(4) 2.7580(18) Å, H(3)···N(4) 2.299(18) Å, N(3)–H(3)···N(4) 112.8(14)° and N(3)···O(8) 2.7607(17) Å, H(3)···O(8) 1.974(19) Å, N(3)–H(3)···O(8) 149.1(16)°]. An intermolecular H-bond further links molecules into chains [N(2)···O(7A) 2.8782(19) Å, H(2)···O(7A) 2.05(2) Å, N(2)–H(2)···O(7A) 161.8(18)° and N(4)···O(8B) 2.8824(17) Å, H(4)···O(8B) 2.067(19) Å, N(4)–H(4)···O(8B) 169.4(17)°. Symmetry operators: *A*: $-x + 1$, $-y$, $-z + 1$, *B*: $-x$, $-y + 1$, $-z$].

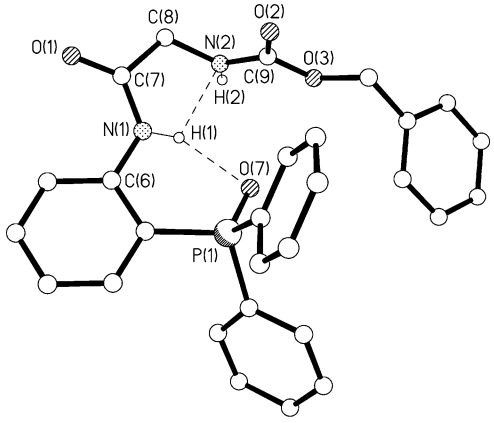

Figure 3. Molecular structure of **2a** showing the bifurcated N(1)–H(1)···N(2) and N(1)–H(1)···O(7) intramolecular H-bonding. All hydrogen atoms except H(1) and H(2) have been omitted for clarity.

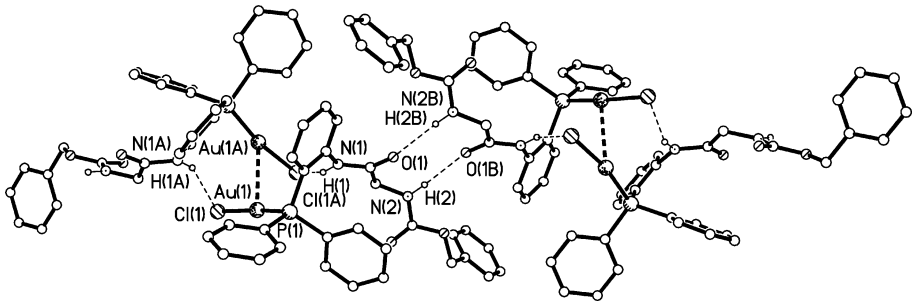

Figure 4. Packing plot of **3** showing those H-atoms involved in H-bonding and the aurophilic interaction. Symmetry operators: A $-x + 1, y, -z + 3/2$, B $-x + 1/2, -y + 1/2, -z + 1$.

Complexation Studies

κ¹-P-Coordination

A range of late transition-metal complexes with **2·HH** were prepared (Scheme 1) either by substitution of a labile ligand (tht for **3**, cod for **8** and **9**) or chloride-bridge cleavage of an organometallic dimer (as in the case of **4**–**7**). All the mononuclear complexes were isolated in good to excellent yields (68–98%) and have been fully characterised by NMR, FT-IR and microanalysis. The $^{31}P\{^{1}H\}$ NMR spectroscopic data for complexes **3**–**9** show the expected downfield shifts upon P-coordination of **2·HH** (see Exp. Sect.).

The X-ray structure of **3** (Figure 4, Table 1) clearly reveals coordination at P of an AuCl unit. The Au–Cl and Au–P bond lengths are normal although the Cl–Au–P bond angle [169.99(3)°] deviates some 10° from the ideal angle expected for a linear geometry.[26,27] This "bending back" can presumably be attributed to the strong aurophilic interaction [3.0926(9) Å] between two molecules of **3** leading to a dimer pair.[27–29] Intermolecular hydrogen bonding between pendant $NHC(O)CH_2NHCO_2Bz$ groups leads to a classic head-to-tail arrangement [N(2)···O(1B) 3.034(4) Å, H(2)···O(1B) 2.17(2) Å, N(2)–H(2)···O(1B) 168(4)°]. The remaining N(H) group within each aurophilic linked dimer is involved in intramolecular N–H···Cl hydrogen bonding [N(1)···Cl(1A) 3.347(3) Å, H(1)···Cl(1A) 2.52(2) Å, N(1)–H(1)···Cl(1A) 152(3)°].

Compound **4**·Et_2O (Figure 5, Table 1) shows a classic piano-stool arrangement about the central Rh^{III} centre comprising a pentahapto coordinated Cp*, two chlorides and a monodentate bound phosphane **2·HH**. Although no unusual structural features were observed there was an intramolecular N–H···Cl hydrogen bond [N(1)···Cl(2) 3.188(8) Å, H(1)···Cl(2) 2.35 Å, N(1)–H(1)···Cl(2) 159°]. This H-bond motif is similar to that found in **3**.

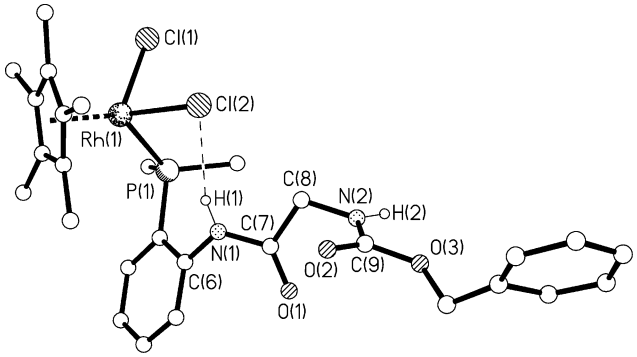

Figure 5. Molecular structure of **4**·Et_2O. The intermolecular H-bonded diethyl ether solvent has been omitted for clarity. Only the phenyl ipso carbons on P(1) are shown.

The X-ray structure of **8** (Figure 6, Table 1) reveals a *trans* stereochemistry of the two phosphane (**2·HH**) ligands. The Pd–Cl [2.2999(8) Å] and Pd–P [2.3288(8) Å] bond

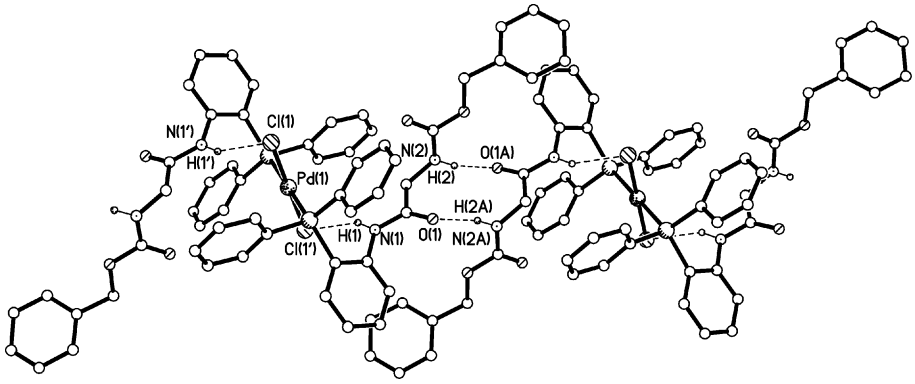

Figure 6. Packing plot of **8** showing the two H-bonding motifs. Symmetry operators: ′: $-x + 1, -y + 1, -z + 1$; A: $-x + 1, -y + 1, -z$.

lengths are normal and compare favourably with other $PdCl_2(PR_3)_2$ complexes with a *trans* disposition.[30] The –NHC(O)CH_2N(H)CO_2Bz dangling groups are clearly positioned above and below the $PdCl_2P_2$ coordination plane. The hydrogen-bonding motif in **8** resembles that previously observed for the Au^I complex **3**. Hence H(1) forms an intramolecular N–H···Cl hydrogen bond [N(1)···Cl(1′) 3.102(3) Å, H(1)···Cl(1′) 2.30(2) Å, N(1)–H(1)···Cl(1′) 152(3)°]. Furthermore, the N(2)–H(2) and an adjacent carbonyl O(1) are involved in hydrogen bonding affording an $R^2_2(10)$ ten-membered ring [N(2)···O(1A) 2.866(4) Å, H(2)···O(1A) 2.01(3) Å, N(2)–H(2)···O(1A) 167(4)°]. Both these H-bonds are stronger than those found in **3**.

κ²-P/N-Coordination

Having established the classic κ¹-P coordination mode that would be expected for the tertiary phosphane **2·HH**, the ease by which this ligand could chelate transition metals forming five-membered M–P–C–C–N metallacycles was explored.[31] Accordingly when compounds **8** or **9** were treated with *t*BuOK in CH_3OH the solids **10** or **11** were isolated in high yields [Equation (1), R = C(O)CH_2NHCO_2Bz]. The Ni^{II} complex **12** was obtained directly from $NiCl_2·6H_2O$, 2 equiv. of **2·HH** and *t*BuOK in refluxing CH_3OH. In all cases the $^{31}P\{^1H\}$ NMR spectra of **10**–**12** showed new downfield phosphorus resonances at δ(P) 19.7 (**10**), 42.2 (**11**) and 21.2 (**12**) ppm. Furthermore, the *J*(PtP) coupling constant for **10** was ca. 400 Hz less than found for **9** in accord with P *trans* to N. Whilst attempts to prepare a clean sample of the single deprotonated chelate complex **13** failed, a few X-ray quality crystals of **13** were obtained and the X-ray structure determined (vide infra).

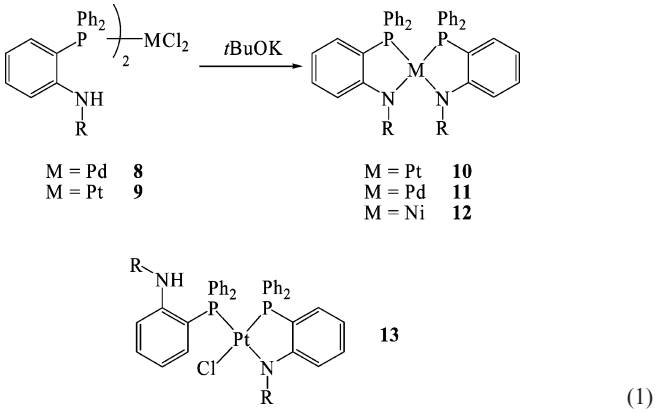

(1)

The X-ray structures of **10**–**12** have each been determined (Figure 7 for compound **10**, Supporting Information for compounds **11** and **12**). All three compounds are isostructural and comprise a central metal chelated by two, *cis*-disposed, κ²-P/N-ligands. The M–P and M–N bond lengths (Table 2) are normal and are similar to previous documented cases.[31] Furthermore, the central metal is displaced by 0.0347 Å (**10**), 0.0341 Å (**11**) and 0.0259 Å (**12**) out of the basal plane of the four donor atoms [P(1), P(2), N(1) and N(3)]. In addition, both five-membered chelate rings in **10**–**12** adopt a conformation best described as envelope with the metal atom at the tip of the flap and with hinge angles [M(1)/P(1)/N(1) vs. N(1)/C(6)/C(1)/P(1) and M(1)/P(2)/N(3) vs. N(2)/C(34)/C(29)/P(2)] in the range 29.4–33.9°. The pendant groups on N(1) and N(3) point away from each other and are involved in different hydrogen bonding arrangements (Supporting Information). Hence H(4) is intramolecular H-bound to O(4) [N···O 2.614(4) Å, 2.23(3) Å, 109(3)° for **10**; N···O 2.619(3) Å, 2.24(3) Å, 110(2)° for **11**; N···O 2.591(3) Å, 2.19(3) Å, 109(2)° for **12**]. In contrast, the C(O) and NH groups of the second chain are involved in intermolecular H-bonding affording dimer pairs [N···O 2.791(4) Å, 2.02(4) Å, 172(4)° for **10**; N···O 2.786(3) Å, 2.00(3) Å, 173(3)° for **11**; N···O 2.800(3) Å, 1.987(18) Å, 173(3)° for **12**].

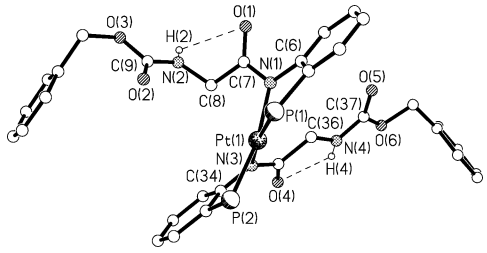

Figure 7. Molecular structure of **10** (compounds **11** and **12** are isostructural and not shown). The phenyl rings on P(1) and P(2) have been removed for clarity.

Table 2. Selected bond lengths [Å] and angles [°] for compounds **10**–**12**.

	10 (M = Pt)	**11** (M = Pd)	**12** (M = Ni)
M(1)–N(1)	2.089(2)	2.0916(17)	1.933(2)
M(1)–N(3)	2.103(2)	2.1127(17)	1.963(2)
M(1)–P(1)	2.2315(8)	2.2420(6)	2.1635(7)
M(1)–P(2)	2.2273(8)	2.2408(6)	2.1602(7)
C(6)–N(1)	1.425(4)	1.421(3)	1.427(3)
N(1)–C(7)	1.355(4)	1.351(3)	1.347(3)
C(7)–O(1)	1.233(3)	1.237(3)	1.232(3)
N(2)–C(9)	1.331(4)	1.334(3)	1.334(4)
C(9)–O(2)	1.218(4)	1.214(3)	1.213(3)
C(9)–O(3)	1.366(4)	1.367(3)	1.360(3)
C(34)–N(3)	1.415(4)	1.415(3)	1.420(3)
N(3)–C(35)	1.367(4)	1.353(3)	1.349(3)
C(35)–O(4)	1.222(4)	1.233(3)	1.232(3)
N(4)–C(37)	1.339(4)	1.340(3)	1.339(3)
C(37)–O(5)	1.209(4)	1.205(3)	1.209(3)
C(37)–O(6)	1.350(4)	1.356(3)	1.352(3)
N(1)–M(1)–N(3)	96.89(9)	98.47(7)	97.05(9)
N(1)–M(1)–P(1)	81.28(7)	81.04(5)	83.21(6)
N(1)–M(1)–P(2)	168.31(7)	167.73(5)	165.77(7)
P(1)–M(1)–P(2)	101.26(3)	100.31(2)	97.93(3)
P(2)–M(1)–N(3)	82.16(7)	82.04(5)	84.59(6)
P(1)–M(1)–N(3)	171.74(7)	171.30(5)	168.74(6)

The X-ray structure of **13**·Et_2O has also been determined (Figure 8, Table 3). The asymmetric unit comprises two molecules of the platinum complex and two molecules of Et_2O (one independent molecule shown in Figure 8). Both molecules display the expected square-planar geometry comprising one κ¹-P-monodentate, a κ²-P/N-didentate and

a chlorido ligand. The Pt lies 0.1197 Å (0.1084 Å for the second independent molecule) out of the basal plane. Both Pt–P distances are similar despite the different *trans* ligands [Pt–P 2.2450(10) and 2.2421(10) Å for P *trans* to Cl; Pt–P 2.2666(11) and 2.2703(11) Å for P *trans* to NR_2]. The Pt–P–C–C–N chelate ring is markedly distorted with hinge angles of 34.0° and 35.5° for the two independent molecules. The NHC(O) hydrogen on the κ^1-P-monodentate bound ligand is intramolecularly H-bonded to the terminal chloride [N···Cl 3.177(4), 3.165(4) Å, H···Cl 2.43(4), 2.38(4) Å, N–H···Cl 155(4), 169(4)°]. Furthermore, within the same group, the NH hydrogen in the $NHCO_2Bz$ group is involved in H-bonding to the Et_2O solvate [N···O 2.972(5), 3.000(5) Å, H···O 2.21(4), 2.18(4) Å, N–H···O 165(5), 169(4)°]. The other chain on the κ^2-P/N-chelate ligand forms a head-to-tail $R^2_2(10)$ H-bonded ring [N···O 2.903(5), 2.973(4) Å, H···O 2.18(4), 2.16(4) Å, N–H···O 166(5), 160(4)°] (Supporting Information).

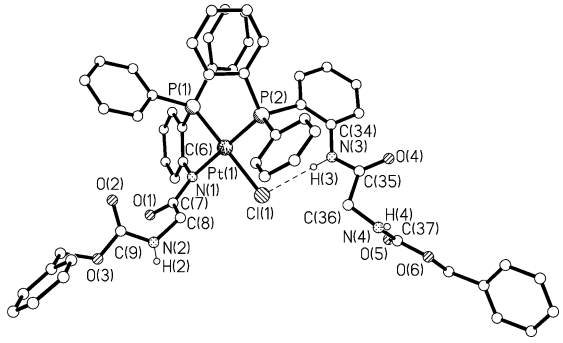

Figure 8. Molecular structure of **13**·Et_2O showing one independent molecule only. The diethyl ether solvent and all hydrogen atoms except those on nitrogen have been omitted for clarity.

Table 3. Selected bond lengths [Å] and angles [°] for compound **13**·Et_2O.

	13·Et_2O[a]
Pt(1)–Cl(1)	2.3761(10) [2.3743(10)]
Pt(1)–P(1)	2.2450(10) [2.2421(10)]
Pt(1)–P(2)	2.2666(11) [2.2702(11)]
Pt(1)–N(1)	2.097(3) [2.088(3)]
C(6)–N(1)	1.423(5) [1.419(5)]
N(1)–C(7)	1.358(5) [1.362(5)]
C(7)–O(1)	1.242(5) [1.234(5)]
N(2)–C(9)	1.335(6) [1.346(6)]
C(9)–O(2)	1.219(6) [1.216(5)]
C(9)–O(3)	1.360(6) [1.361(5)]
C(34)–N(3)	1.411(5) [1.414(5)]
N(3)–C(35)	1.362(5) [1.358(5)]
C(35)–O(4)	1.213(5) [1.214(5)]
N(4)–C(37)	1.346(6) [1.345(5)]
C(37)–O(5)	1.210(5) [1.210(5)]
C(37)–O(6)	1.361(5) [1.360(5)]
Cl(1)–Pt(1)–N(1)	90.21(9) [89.58(9)]
Cl(1)–Pt(1)–P(1)	163.75(4) [164.42(4)]
Cl(1)–Pt(1)–P(2)	89.22(4) [90.16(4)]
P(1)–Pt(1)–P(2)	100.29(4) [100.18(4)]
P(1)–Pt(1)–N(1)	80.60(9) [80.27(9)]
P(2)–Pt(1)–N(1)	178.45(9) [179.02(9)]

[a] Two independent molecules in the asymmetric unit.

κ^3-P/N/N′-Coordination

To evaluate whether **2·HH** could function effectively as a tridentate system, the Ir^{III} complex **5** was treated with *t*BuOK in refluxing CH_3OH [Equation (2)]. The $^{31}P\{^1H\}$ NMR spectrum of the crude material revealed two new phosphorus signals at δ(P) 16.0 and 8.0 ppm in a 1.0:3.2 ratio. Both phosphorus resonances are assigned to the two diastereomers of the chiral-at-metal complex Ir(η^5-Cp*){2-$Ph_2PC_6H_4NC(O)CH_2NCO_2Bz$} (**14**) containing a κ^3-dianionic P/N/N′ ligand. Similarly the Ru^{II} complex **6** gave, under similar conditions, the chiral-at-metal complex Ru(η^6-*p*-cymene){2-$Ph_2PC_6H_4NC(O)CH_2NCO_2Bz$} (**15**) in 80% isolated yield. The $^{31}P\{^1H\}$ NMR spectrum of **15** showed two new signals at δ(P) 50.2 and 46.6 ppm, in an approximate 1.0:1.0 ratio, consistent with the presence of two diastereomers. Other characterising data are given in the Exp. Sect.

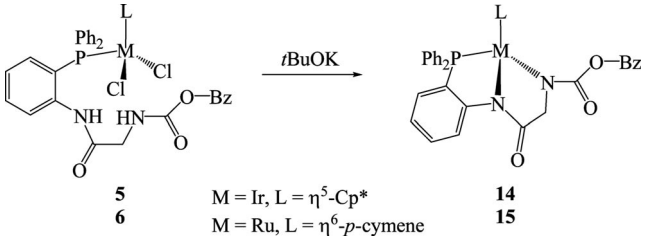

(2)

In order to establish unambiguously the coordination mode of **2** we were fortunate to obtain a few crystals of **14** which indeed confirmed κ^3-P/N/N′-coordination. The X-ray structure of **14** (Figure 9, Table 4) confirms this tridentate coordination mode for **2**. The ligand chelates forming two five-membered rings, Ir(1)–P(1)–C(1)–C(6)–N(1) and Ir(1)–N(2)–C(8)–C(7)–N(1), that display hinge angles of 30.4° [Ir(1)/P(1)/N(1) vs. P(1)/C(1)/C(6)/N(1)] and 25.3° [Ir(1)/N(1)/N(2) vs. N(1)/C(7)/C(8)/N(2)]. The Ir(1)–P(1) length is in the range typically expected[32] and the Ir(1)–N(1)/N(2) distances are very similar. There are significant differences between the P(1)–Ir(1)–N(1) [76.4(2)°] and P(1)–

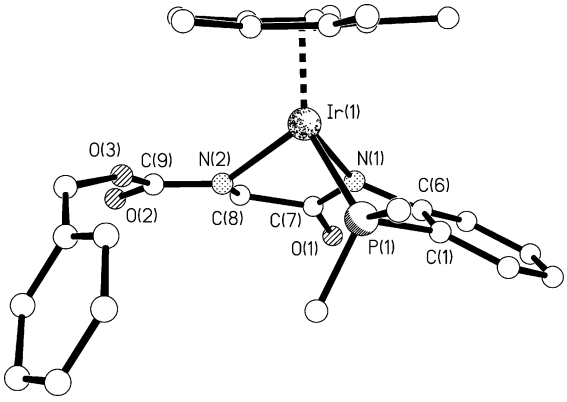

Figure 9. Molecular structure of **14** showing the major disorder component only. All hydrogen atoms removed for clarity. Only the phenyl *ipso* carbon atoms on P(1) are shown.

Ir(1)–N(2) [97.5(3)°] bond angles presumably as a consequence of the differing phenyl vs. alkyl backbones separating the P/N donor atoms. Within the Ir(1)–N(2)–C(8)–C(7)–N(1) ring the Ir(1), N(1), C(7), C(8) atoms are co-planar to within ±0.03 Å whilst N(2) is the flap of an envelope lying 0.58 Å out of this plane. For the other five-membered ring, N(1), C(6), C(1) and P(1) are co-planar to within ±0.02 Å whilst Ir(1) lies 0.98 Å out of this plane.

Table 4. Selected bond lengths [Å] and angles [°] for compound **14**.

	14[a]
Ir(1)–P(1)	2.271(2)
Ir(1)–N(1)	2.085(8)
Ir(1)–N(2)	2.082(9)
Ir(1)–$C_{centroid}$	1.8459(42)
C(6)–N(1)	1.409(11)
N(1)–C(7)	1.368(13)
C(7)–O(1)	1.232(12)
N(2)–C(9)	1.29(2)
C(9)–O(2)	1.37(2)
C(9)–O(3)	1.22(2)
P(1)–Ir(1)–N(1)	76.4(2)
P(1)–Ir(1)–N(2)	97.5(3)
N(1)–Ir(1)–N(2)	77.0(4)
C(6)–N(1)–C(7)	120.0(8)
N(1)–C(7)–O(1)	125.2(10)
N(2)–C(9)–O(2)	120.7(15)
O(2)–C(9)–O(3)	120.0(16)

[a] Major component.

Conclusions

In summary, we have shown that a new P/N/N′-functionalised ligand **2·HH** can display various coordination modes dependant on the geometry of the transition-metal centre (linear, square-planar or pseudo-tetrahedral). This flexibility in ligand geometry mirrors our previous studies with a P/N/N′/N′′-tetradentate system which likewise can adopt numerous coordination motifs.[25] The amide functional groups adopt various secondary hydrogen-bonding interactions and in solution, we believe some of these compounds exist as conformers due to hindered amide-bond rotation. Further studies are in progress and will be reported in due course.

Experimental Section

Materials: All reactions were carried out in air with the exception of **2·HH** whose synthesis was conducted under dry, oxygen-free nitrogen. All solvents were distilled prior to use. The compound 2-$Ph_2PC_6H_4(NH_2)$ (**1**) was a kind donation from Dr S. M. Aucott whereas AuCl(tht) (tht = tetrahydrothiophene),[33] MCl_2(cod) (M = Pt, Pd; cod = cycloocta-1,5-diene),[34] $\{RuCl_2(\eta^6\text{-}p\text{-cymene})\}_2$,[35] $\{MCl_2(\eta^5\text{-Cp*})\}_2$ (M = Rh, Ir)[36] and $\{PdCl(\kappa^2\text{-CN-}C_{12}H_{12}N)\}_2$[37] were prepared according to published procedures. All other reagents were purchased from commercial suppliers and used directly without further purification.

Instrumentation: FT-IR spectra were recorded as KBr pellets over the range 4000–200 cm^{-1} using a Perkin–Elmer system 2000 FT spectrometer. ^1H NMR and $^{31}P\{^1H\}$ NMR spectra (298 ± 2 K) were recorded either with Bruker AC250 or DPX-400 FT spectrometers with chemical shifts (δ) reported relative to external TMS or H_3PO_4. All NMR spectra (250 or 400 MHz) were recorded in $CDCl_3$ solutions unless otherwise stated. Elemental analyses (Perkin–Elmer 2400 CHN Elemental Analyzer) were performed by the Loughborough University Analytical Service within the Department of Chemistry.

Preparation of 2-$Ph_2PC_6H_4NHC(O)CH_2NHCO_2Bz$, (2·HH): A solution of **1** (2.003 g, 7.222 mmol), *N*-(benzyloxycarbonyl)glycine (1.511 g, 7.222 mmol) and 1,3-dicyclohexylcarbodiimide, DCC, (1.594 g, 7.725 mmol) in THF (60 mL) was stirred at ambient temperature, under nitrogen for 4 d. The solid was removed by filtration, washed with some THF and the combined filtrate evaporated to dryness. The residue was taken up in CH_2Cl_2 (25 mL), passed through a small plug and Et_2O (80 mL) added. The solid **2·HH** was collected by suction filtration, washed with a small portion of Et_2O and dried. Yield 1.217 g, 36%. Selected data: ^{31}P NMR ($CDCl_3$): δ = –20.7, –21 .3 (ratio 8.0:1.0) ppm. ^1H NMR ($CDCl_3$): δ = 8.45 (s, 1 H, arom. H), 8.14 (m, 1 H, arom. H), 7.37–7.26 (m, 15 H, arom. H), 7.08 (t, 1 H, arom. H), 6.92 (dt, 1 H, arom. H), 5.12 (s, 3 H, overlapping OCH_2 and NH), 3.79 (d, ^3J = 4 Hz, 2 H, NCH_2) ppm. FT-IR (KBr): $\tilde{\nu}$ = 3328, 3264 (NH), 1721 (CO), 1677 (amide I), 1522 (amide II) cm^{-1}. EI-MS: *m*/*z* = 468 [M^+]. $C_{28}H_{25}N_2O_3P$ (468.5): calcd. C 71.78, H 5.39, N 5.98; found C 71.67, H 5.18, N 5.77.

2-$Ph_2P(O)C_6H_4NHC(O)CH_2NHCO_2Bz$ (2a): The tertiary phosphane oxide was prepared by oxidation of **2·HH** (0.040 g, 0.085 mmol) with aq. H_2O_2 (27.5% w/w, 6 drops) in $CDCl_3$. Yield 0.027 g, 66%. Selected data: ^{31}P NMR ($CDCl_3$): δ = 37.2, 36.9 (ratio 1:5.4) ppm. ^1H NMR ($CDCl_3$): δ = 11.30 (s, 1 H, NH), 8.47 (m, 1 H, arom. H), 7.61–6.90 (m, 18 H, arom. H), 5.40 (t, 1 H, NH), 5.06 (s, 2 H, OCH_2), 3.92 (d, ^3J = 4 Hz, 2 H, NCH_2) ppm. FT-IR (KBr): $\tilde{\nu}$ = 3255 (NH), 1720 (CO), 1712, 1694 (amide I), 1536 (amide II) 1153 (PO) cm^{-1}. ES-MS: *m*/*z* = 485 [M + H^+]. $C_{28}H_{25}N_2O_4P$ (484.5): calcd. C 69.41, H 5.21, N 5.78; found C 69.40, H 5.21, N 5.70.

Preparation of AuCl{2-$Ph_2PC_6H_4NHC(O)CH_2NHCO_2Bz$} (3): **2·HH** (0.103 g, 0.220 mmol) was added to a CH_2Cl_2 (10 mL) solution of AuCl(tht) (0.071 g, 0.22 mmol). The colourless solution was stirred for 20 min, concentrated under reduced pressure to ca. 1–2 mL and Et_2O (20 mL) and hexanes (20 mL) added. The solid **3** was collected by suction filtration and dried. Yield 0.147 g, 95%. Selected data: ^{31}P NMR ($CDCl_3$): δ = 20.9 ppm. ^1H NMR ($CDCl_3$): δ = 8.30 (s, 1 H, NH), 7.96 (m, 1 H, arom. H), 7.56–6.80 (m, 18 H, arom. H), 5.42 (br., 1 H, NH), 5.08 (s, 2 H, OCH_2), 3.81 (d, ^3J = 6 Hz, 2 H, NCH_2) ppm. FT-IR (KBr): $\tilde{\nu}$ = 3362, 3274 (NH), 1724 (CO), 1691 (amide I), 1506 (amide II), 318 (AuCl) cm^{-1}. ES-MS: *m*/*z* = 665 [M – Cl]. $C_{28}H_{25}AuClN_2O_3P$ (700.9): calcd. C 47.98, H 3.60, N 4.00; found C 48.12, H 3.36, N 3.88.

Preparation of Ir(η^5-Cp*)Cl_2\{2-$Ph_2PC_6H_4NHC(O)CH_2NHCO_2Bz$\} (5): **2·HH** (0.072 g, 0.154 mmol) was added to a CH_2Cl_2 (10 mL) solution of $\{IrCl_2(\eta^5\text{-Cp*})\}_2$ (0.061 g, 0.077 mmol). The orange solution was stirred for 20 min, passed through a small plug, concentrated under reduced pressure to ca. 1–2 mL and Et_2O (10 mL) added. The solid **5** was collected by suction filtration and dried. Yield 0.130 g, 98%. Selected data: ^{31}P NMR ($CDCl_3$): δ = 0.0, –0.2 (ratio 4.0:1) ppm. ^1H NMR ($CDCl_3$): δ = 8.80 (s, 1 H, arom. H), 7.85–6.81 (m, 17 H, arom. H), 5.07 (br., 1 H, NH), 4.95, 4.91 (both s, 2 H, OCH_2), 3.83, 2.99 (both br., 2 H, NCH_2), 1.22 (d, ^4J = 2 Hz, 15 H, Cp*) ppm. FT-IR (KBr): $\tilde{\nu}$ = 3282, 3242, 3226, 3211 (NH), 1729 (CO), 1710 (amide I), 1514 (amide II) cm^{-1}. ES-MS:

m/*z* = 795 [M – 2 Cl – H]. $C_{38}H_{40}Cl_2IrN_2O_3P$ (867.6): calcd. C 52.65, H 4.66, N 3.23; found C 52.82, H 4.85, N 2.88.

Rh(η⁵-Cp*)Cl₂{2-Ph₂PC₆H₄NHC(O)CH₂NHCO₂Bz} (4): The rhodium(III) complex was prepared from **2·HH** and $\{RhCl_2(\eta^5\text{-}Cp^*)\}_2$ (89%). Selected data: ^{31}P NMR ($CDCl_3$): δ = 27.4 [*J*(RhP) = 143 Hz], 27.2 [*J*(RhP) = 143 Hz] (ratio 3.0:1.0) ppm. ^1H NMR ($CDCl_3$): δ = 9.24 (s, 1 H, arom. H), 8.07–6.99 (m, 17 H, arom. H), 5.22 (br., 1 H, NH), 5.10, 5.06 (both s, 2 H, OCH_2), 3.88, 3.05 (both br., 2 H, NCH_2), 1.40 (d, ^4J = 3.6 Hz, 15 H, Cp*) ppm. FT-IR (KBr): $\tilde{\nu}$ = 3237, 3194, (NH), 1726 (CO), 1706 (amide I), 1509 (amide II) cm^{-1}. ES-MS: *m*/*z* = 705 [M – 2 Cl – H]. $C_{38}H_{40}Cl_2N_2O_3PRh{\cdot}0.5CH_2Cl_2$ (820.0): calcd. C 56.39, H 5.05, N 3.42; found C 56.18, H 5.08, N 3.34.

Preparation of Ru(η⁶-*p*-cymene)Cl₂{2-Ph₂PC₆H₄NHC(O)CH₂-NHCO₂Bz} (6): 2·HH (0.098 g, 0.21 mmol) was added to a CH_2Cl_2 (10 mL) solution of $\{RuCl_2(\eta^6\text{-}p\text{-cymene})\}_2$ (0.064 g, 0.10 mmol). The orange solution was stirred for 15 min and concentrated under reduced pressure to ca. 1–2 mL. Addition of Et_2O (10 mL) gave **6** which was collected by suction filtration and dried. Yield 0.146 g, 90%. Selected data: ^{31}P NMR ($CDCl_3$): δ = 24.3, 23.7 (ratio 5.5:1.0) ppm. ^1H NMR ($CDCl_3$): δ = 8.89 (s, 1 H, arom. H), 8.01 (m), 7.88–7.08 (m), 5.30–4.89 (m, *p*-cymene, OCH_2, NCH_2), 2.89 (sept., 1 H, CH), 1.87 (s, 3 H, CH_3), 1.24 [br, 6 H, $CH(CH_3)_2$] ppm. FT-IR (KBr): $\tilde{\nu}$ = 3365, 3237, 3208 (NH), 1730 (CO), 1704 (amide I), 1522 (amide II) cm^{-1}. ES-MS: *m*/*z* = 775 [M]. $C_{38}H_{39}Cl_2N_2O_3$-PRu (774.7): calcd. C 58.91, H 5.08, N 3.62; found C 58.76, H 4.94, N 3.51.

Preparation of Pd(κ²-CN-C₁₂H₁₂N)Cl{2-Ph₂PC₆H₄NHC(O)CH₂-NHCO₂Bz} (7): 2·HH (0.121 g, 0.258 mmol) was added to a CH_2Cl_2 (20 mL) solution of $\{PdCl(\kappa^2\text{-}CN\text{-}C_{12}H_{12}N)\}_2$ (0.079 g, 0.13 mmol). The yellow solution was stirred for 30 min and concentrated under reduced pressure to ca. 1–2 mL. Addition of Et_2O (10 mL) and petroleum ether (b.p. 60–80 °C, 20 mL) gave **7** which was collected by suction filtration and dried. Yield 0.134 g, 68%. Selected data: ^{31}P NMR ($CDCl_3$): δ = 38.8 ppm. ^1H NMR ($CDCl_3$): δ = 9.17 (s, 1 H, arom. H), 7.83–6.81 (m, 23 H, arom. H), 6.61 (t, 1 H, arom. H), 6.45 (t, 1 H, arom. H), 5.21 (br., 1 H, NH), 4.94 (s, 2 H, OCH_2), 3.54 (d, *J* = 2.8 Hz, 2 H, NCH_2), 3.42 (s, 6 H, CH_3) ppm. FT-IR (KBr): $\tilde{\nu}$ = 3420, 3297 (NH), 1725 (CO), 1691 (amide I), 1498 (amide II) cm^{-1}. ES-MS: *m*/*z* = 745 [M – Cl]. $C_{40}H_{37}ClN_3O_3PPd$ (780.6): calcd. C 61.54, H 4.79, N 5.38; found C 61.64, H 4.38, N 5.05.

Preparation of $PdCl_2${2-Ph₂PC₆H₄NHC(O)CH₂NHCO₂Bz}₂ (8): 2·HH (0.226 g, 0.482 mmol) was added to a CH_2Cl_2 (20 mL) solution of $PdCl_2$(cod) (0.069 g, 0.24 mmol). The yellow solution was stirred for ca. 1 h and concentrated under reduced pressure to ca. 1–2 mL. Addition of Et_2O (10 mL) and hexanes (10 mL) gave **8** which was collected by suction filtration and dried. Yield 0.260 g, 97%. Selected data: ^{31}P NMR ($CDCl_3$): δ = 19.9, 19.1 ppm. ^1H NMR ($CDCl_3$): δ = 8.43 (s, 2 H, arom. H), 7.75–7.06 (m, 38 H, arom. H), 5.24 (br., 2 H, NH), 5.03 (s, 4 H, OCH_2), 3.35 (br., 4 H, NCH_2) ppm. FT-IR (KBr): $\tilde{\nu}$ = 3312 (NH), 1724 (CO), 1700 (amide I), 1506 (amide II) cm^{-1}. ES-MS: *m*/*z* = 1041 [M – 2 Cl – H]. $C_{56}H_{50}Cl_2N_4O_6P_2Pd$ (1114.3): calcd. C 60.36, H 4.53, N 5.03; found C 60.25, H 4.17, N 4.77.

$PtCl_2${2-Ph₂PC₆H₄NHC(O)CH₂NHCO₂Bz}₂ (9): This compoound was prepared from $PtCl_2$(cod) and two equiv. of **2·HH** (91%). Selected data: ^{31}P NMR ($CDCl_3$): δ = 6.7 [*J*(PtP) = 3657 Hz] (major species) ppm. ^1H NMR ($CDCl_3$): δ = 9.23 (s, 2 H, arom. H), 7.78–6.77 (m, 38 H, arom. H), 5.60 (br., 2 H, NH), 5.10 (s, 4 H, OCH_2), 3.79 (br., 4 H, NCH_2) ppm. FT-IR (KBr): $\tilde{\nu}$ = 3377 (NH), 1718 (CO and amide I), 1498 (amide II) cm^{-1}. ES-MS: *m*/*z* = 1131 [M – 2 Cl – H]. $C_{56}H_{50}Cl_2N_4O_6P_2Pt$ (1203.0): calcd. C 55.91, H 4.20, N 4.66; found C 55.84, H 3.82, N 4.48.

Preparation of *cis*-Pd{2-Ph₂PC₆H₄NC(O)CH₂NHCO₂Bz}₂ (11): *t*BuOK (0.035 g, 0.31 mmol) was added to a CH_3OH (5 mL) suspension of **8** (0.125 g, 0.112 mmol) to give a yellow solution followed by the immediate formation of a yellow solid. The mixture was refluxed for 3 h and left to cool overnight. The solid **11** was collected by suction filtration, washed with a small portion of CH_3OH and dried. Yield 0.103 g, 88%. Selected data: ^{31}P NMR ($CDCl_3$): δ = 42.2 ppm. ^1H NMR ($CDCl_3$): δ = 8.04 (m, 2 H, arom. H), 7.43–6.91 (m, 36 H, arom. H), 5.73 (br., 2 H, NH), 5.08 (s, 4 H, OCH_2), 4.33 (m, 4 H, NCH_2) ppm. FT-IR (KBr): $\tilde{\nu}$ = 3377 (NH), 1718 (CO and amide I), 1498 (amide II) cm^{-1}. ES-MS: *m*/*z* = 1131 [M – 2 Cl – H]. $C_{56}H_{48}N_4O_6P_2Pd$ (1041.4): calcd. C 64.59, H 4.66, N 5.38; found C 63.78, H 4.68, N 5.24.

***cis*-Pt{2-Ph₂PC₆H₄NC(O)CH₂NHCO₂Bz}₂ (10):** This complex was likewise prepared from **9** (88%). Selected data: ^{31}P NMR ($CDCl_3$): δ = 19.7 [*J*(PtP) = 3217 Hz] ppm. FT-IR (KBr): $\tilde{\nu}$ = 3377 (NH), 1718 (CO and amide I), 1498 (amide II) cm^{-1}. ES-MS: *m*/*z* = 1130 [M^+]. $C_{56}H_{48}N_4O_6P_2Pt$ (1130.1): calcd. C 59.52, H 4.29, N 4.96; found C 59.08, H 3.96, N 4.77.

Preparation of *cis*-Ni{2-Ph₂PC₆H₄NC(O)CH₂NHCO₂Bz}₂ (12): A mixture of $NiCl_2{\cdot}6H_2O$ (0.025 g, 0.11 mmol), **2·HH** (0.103 g, 0.220 mmol) and *t*BuOK (0.035 g, 0.32 mmol) in CH_3OH (10 mL) was refluxed for 3 h. The mixture was left to stand to deposit an orange crystalline material that was collected by filtration under suction and dried. Yield 0.022 g, 21%. Selected data: ^{31}P NMR ($CDCl_3$): δ = 21.2 ppm. FT-IR (KBr): $\tilde{\nu}$ = 3377, 3245 (NH), 1714 (CO and amide I) cm^{-1}. ES-MS: *m*/*z* = 993 [M]. $C_{56}H_{48}N_4NiO_6P_2$ (993.7): calcd. C 67.70, H 4.88, N 5.64; found C 67.74, H 4.84, N 5.37.

Preparation of Ir(η⁵-Cp*){2-Ph₂PC₆H₄NC(O)CH₂NCO₂Bz} (14): A mixture of **5** (0.029 g, 0.033 mmol) and *t*BuOK in CH_3OH (5 mL) was refluxed, under nitrogen for 3 h. The solution was cooled and the solvents evaporated to dryness under reduced pressure. Examination of the crude mixture revealed two new major species at δ(P) = 16.0 and 8.0 ppm in a 1:3.2 ratio. Crystallisation was achieved using $CDCl_3$/petroleum ether (b.p. 60–80 °C) to give a small quantity of crystalline material identified as **14**. Selected data: ^{31}P NMR (C_6D_6): δ = 17.7, 8.8 (ratio 1.4:1.0) ppm. ^1H NMR (C_6D_6): δ = 8.66 (dd, 1 H, arom. H), 8.60 (dd, 1 H, arom. H), 8.03 (m, 1 H, arom. H), 7.80 (m, 1 H, arom. H), 7.63–6.72 (m, 34 H, arom. H), 5.64 (d, *J* = 17.6 Hz, 1 H, CH_2), 5.44 (dd, 2 H, CH_2), 5.09 (d, *J* = 11.6 Hz, 1 H, CH_2), 4.96 (d, *J* = 17.6 Hz, 1 H, CH_2), 4.87 (d, *J* = 11.2 Hz, 1 H, CH_2), 4.44 (d, *J* = 17.6 Hz, 1 H, CH_2), 4.28 (d, *J* = 17.2 Hz, 1 H, CH_2), 1.30 (d, *J* = 2.4 Hz, 15 H, Cp*), 1.08 (d, *J* = 2.0 Hz, 15 H, Cp*) ppm. FT-IR (KBr): $\tilde{\nu}$ = 1658, 1626 (CO and amide I) cm^{-1}. ES-MS: *m*/*z* = 795 [M + H]$^+$. $C_{37}H_{38}Ir$-N_2O_3P (781.9): calcd. C 56.83, H 4.91, N 3.58; found C 56.69, H 4.71, N 3.45.

Preparation of Ru(η⁶-*p*-cymene){2-Ph₂PC₆H₄NC(O)CH₂NCO₂Bz} (15): A mixture of **6** (0.071 g, 0.092 mmol) and *t*BuOK (0.027 g, 0.24 mmol) in CH_3OH (10 mL) was stirred at room temperature for ca. 4 h then refluxed, under nitrogen for 2 h. The solution was cooled and the solvents evaporated to dryness under reduced pressure. The crude material was taken up in CH_2Cl_2 (10 mL) and passed through a Celite plug. The volume was concentrated under reduced pressure to 1–2 mL and diethyl ether (10 mL)/hexanes (10 mL) added. The precipitate was left to stand overnight, filtered and dried in vacuo to give **15**. Yield 0.051 g, 80%. Selected data: ^{31}P NMR ($CDCl_3$): δ = 50.2, 46.6 (ratio 1.0:1.0) ppm. ^1H NMR ($CDCl_3$): δ = 7.73 (dd, 1 H, arom. H), 7.65 (dd, 1 H, arom. H),

7.44–6.97 (m, 34 H, arom. H), 6.85 (t, 1 H, arom. H), 6.78 (t, 1 H, arom. H), 5.16–4.66 (m, 12 H, *p*-cymene, CH_2), 3.97 (d, 1 H, CH_2), 3.80 (d, 1 H, CH_2), 3.72 (dd, 2 H, CH_2), 2.38 (sept., 1 H, CH), 2.06 (sept., 1 H, CH), 1.79 (s, 3 H, CH_3), 1.47 (s, 3 H, CH_3), 0.98 [d, J = 6.8 Hz, 3 H, $CH(CH_3)_2$], 0.91 [d, J = 6.8 Hz, 3 H, $CH(CH_3)_2$], 0.77 [dd, J = 6.8 Hz, 6 H, $CH(CH_3)_2$] ppm. FT-IR (KBr): $\tilde{\nu}$ = 1647, 1619 (CO and amide I) cm^{-1}. EI-MS: m/z = 702 $[M]^+$. $C_{38}H_{37}N_2O_3PRu{\cdot}H_2O$ (720.7): calcd. C 63.32, H 5.47, N 3.89; found C 62.97, H 4.96, N 3.71.

X-ray Crystallography: Suitable crystals were grown by vapour diffusion of diethyl ether into either a CH_2Cl_2 (for **4**·Et_2O, **10**, **11**) or $CDCl_3$ (for **2a**, **3**, **8**) solution. Crystals of **14** were obtained by layering petroleum ether (b.p. 60–80 °C) over a $CDCl_3$ solution. Slow evaporation to dryness of a CH_2Cl_2/Et_2O filtrate from the reaction of $[PtCl_2(cod)]$/1 equiv. **2·HH** (for **13**·Et_2O) or $CDCl_3/Et_2O$ solution (for **2·HH**) afforded suitable X-ray quality crystals. A warm solution of $NiCl_2{\cdot}6H_2O$, **2·HH** and *t*BuOK in CH_3OH was cooled over 2 d to give suitable crystals of **12**. Measurements were made with either a Bruker AXS SMART 1000 CCD area-detector diffractometer[38] for **2·HH**, **2a**, **4**·Et_2O, **10**–**12**, **13**·Et_2O and **14** using sealed-tube graphite-monochromated Mo-K_α radiation and narrow frame exposures (0.3°) in ω or a Bruker-Nonius 95-mm CCD kappa diffractometer[39,40] equipped with a rotating-anode generator for **3** and **8**. Cell parameters were refined from the observed (ω) angles of all strong reflections in each data set. Intensities were corrected semiempirically for absorption, based on symmetry-equivalent and repeated reflections. The structures were solved by

Table 5. Crystallographic data for **2·HH**, **2a**, **3**, **4**·Et_2O and **8**.

Compound	**2·HH**	**2a**	**3**	**4**·Et_2O	**8**
Empirical formula	$C_{28}H_{25}N_2O_3P$	$C_{28}H_{25}N_2O_4P$	$C_{28}H_{25}AuClN_2O_3P$	$C_{42}H_{50}Cl_2N_2O_4PRh$	$C_{56}H_{50}Cl_2N_4O_6P_2Pd$
Formula weight	468.47	484.47	700.89	851.62	1114.24
Crystal system	orthorhombic	triclinic	monoclinic	orthorhombic	triclinic
Space group	*Pbca*	$P\bar{1}$	*C*2/*c*	$P2_12_12_1$	$P\bar{1}$
a [Å]	9.7453(6)	10.0621(5)	22.952(5)	8.4053(3)	9.8211(2)
b [Å]	17.9907(11)	13.8305(6)	12.739(3)	17.2229(7)	12.3556(3)
c [Å]	26.6542(17)	18.7642(9)	17.885(4)	28.0623(12)	13.4933(3)
α [°]		95.1715(8)			73.3569(15)
β [°]		93.9950(8)	94.44(3)		69.6192(15)
γ [°]		110.7979(8)			68.1251(11)
Volume [Å^3]	4673.1(5)	2416.7(2)	5213.6(18)	4062.4(3)	1401.06(5)
Z	8	4	8	4	1
T [K]	150(2)	150(2)	120(2)	150(2)	120(2)
Density (calcd.) [Mg/m^3]	1.332	1.332	1.786	1.392	1.321
Absorption coeff. [mm^{-1}]	0.151	0.152	5.840	0.634	0.534
Crystal	plate, colourless	block, colourless	block, colourless	block, orange	plate, yellow
Crystal size [mm^3]	0.71 × 0.10 × 0.06	0.52 × 0.32 × 0.14	0.28 × 0.14 × 0.06	0.56 × 0.32 × 0.13	0.28 × 0.10 × 0.04
θ Range [°]	2.26–29.05	1.59–29.16	2.98–27.49	1.45–28.99	3.18–27.50
Reflections collected	38962	21740	26325	35012	29162
Independent reflections	5816	11284	5958	9701	6423
	[R_{int} = 0.0578]	[R_{int} = 0.0172]	[R_{int} = 0.0566]	[R_{int} = 0.0404]	[R_{int} = 0.1545]
Final *R*, R_w	0.0452, 0.1049	0.0392, 0.0992	0.0281, 0.0637	0.0775, 0.1800	0.0589, 0.1593

Table 6. Crystallographic data for **10**–**12**, **13**·Et_2O and **14**.

Compound	**10**	**11**	**12**	**13**·Et_2O	**14**
Empirical formula	$C_{56}H_{48}N_4O_6P_2Pt$	$C_{56}H_{48}N_4O_6P_2Pd$	$C_{56}H_{48}N_4NiO_6P_2$	$C_{60}H_{59}ClN_4O_7P_2Pt$	$C_{38}H_{38}IrN_2O_3P$
Formula weight	1130.01	1041.32	993.63	1240.59	793.87
Crystal system	triclinic	triclinic	triclinic	triclinic	orthorhombic
Space group	$P\bar{1}$	$P\bar{1}$	$P\bar{1}$	$P\bar{1}$	*Pbca*
a [Å]	10.9838(5)	10.9942(6)	10.8720(6)	13.0842(5)	14.5434(6)
b [Å]	12.0189(6)	12.0245(6)	12.0122(6)	18.0484(7)	19.0261(9)
c [Å]	18.9373(9)	18.9440(10)	18.9051(10)	25.0130(9)	24.0410(11)
α [°]	86.5717(8)	86.3778(9)	84.0006(10)	109.3285(6)	
β [°]	75.4249(7)	75.5354(9)	75.6778(9)	91.6609(6)	
γ [°]	89.6824(8)	89.6384(9)	89.4411(9)	98.6980(6)	
Volume [Å^3]	2415.1(2)	2420.0(2)	2378.8(2)	5489.9(4)	6652.2(5)
Z	2	2	2	4	8
T [K]	150(2)	150(2)	150(2)	150(2)	150(2)
Density (calcd.) [Mg/m^3]	1.554	1.429	1.387	1.501	1.585
Absorption coeff. [mm^{-1}]	3.028	0.506	0.533	2.720	4.102
Crystal	block, colourless	block, yellow	block, orange	block, colourless	block, yellow
Crystal size [mm^3]	0.35 × 0.16 × 0.13	0.43 × 0.34 × 0.16	0.28 × 0.16 × 0.07	0.42 × 0.34 × 0.11	0.23 × 0.22 × 0.15
θ Range [°]	1.70–29.02	1.70–29.00	1.70–29.08	1.23–25.00	1.69–25.00
Reflections collected	21653	21527	21340	40463	45915
Independent reflections	11226	11181	11032	19293	5877
	[R_{int} = 0.0255]	[R_{int} = 0.0216]	[R_{int} = 0.0324]	[R_{int} = 0.0269]	[R_{int} = 0.0470]
Final *R*, R_w[a]	0.0300, 0.0585	0.0338, 0.0783	0.0457, 0.1083	0.0302, 0.0677	0.0471, 0.1307

[a] $R = \Sigma||F_o| - |F_c||/\Sigma|F_o|$ for "observed" reflections having $F^2 > 2\sigma(F^2)$. $R_w = [\Sigma w(F_o^2 - F_c^2)^2/\Sigma_w(F_o^2)^2]^{1/2}$ for all data.

direct methods (Patterson synthesis for **10** and **11**) and refined on F^2 values for all unique data by full-matrix least-squares.[41] Table 5 and Table 6 give further details. All non-hydrogen atoms were refined anisotropically. For **14** the C(11) > C(16) ring is common to both disorder components and there are two possible conformations of the linkage between this ring and N(2): 56.0(11)% of the time via C(9), O(3), C(10) and 44.0(11)% of the time via C(9X), O(3X), C(10X). For compound **4**·Et_2O a molecule of badly disorderd Et_2O was modelled by the Platon Squeeze procedure.[42] The X-ray structures of **11** (Figure S1) and **12** (Figure S2), with full atom numbering schemes, are given in the Supporting Information.

CCDC-706564 (for **2**·**HH**), -706565 (for **2a**), -706566 (for **3**), -706567 (for **4**·Et_2O), -706568 (for **8**), -706569 (for **10**), -706570 (for **11**), -706571 (for **12**), -706572 (for **13**·Et_2O) and -706573 (for **14**) contain the complete set of X-ray crystallographic structural data. These can be obtained free of charge from The Cambridge Crystallographic Data Centre via www.ccdc.cam.ac.uk/data_request/cif.

Supporting Information (see also the footnote on the first page of this article): Four figures showing additional crystal structures, packing plots, and full atom numbering.

Acknowledgments

We should like to thank the Engineering and Physical Sciences Research Council (EPSRC) X-ray Service at Southampton University for collecting the data set for compounds **3** and **8**, Johnson Matthey for the generous loan of precious metal salts and the EPSRC Mass Spectrometry Service Centre at Swansea. We also acknowledge the Engineering and Physical Sciences Research Council (EPSRC) for partial funding (A. J. L.).

[1] S. Sen, P. Talukder, S. K. Dey, S. Mitra, G. Rosair, D. L. Hughes, G. P. A. Yap, G. Pilet, V. Gramlich, T. Matsushita, *Dalton Trans.* **2006**, 1758–1767.

[2] S. Akine, A. Akimoto, T. Shiga, H. Oshio, T. Nabeshima, *Inorg. Chem.* **2008**, *47*, 875–885.

[3] S. Nag, P. Gupta, R. J. Butcher, S. Bhattacharya, *Inorg. Chem.* **2004**, *43*, 4814–4816.

[4] J. E. Reed, A. Arola Arnal, S. Neidle, R. Vilar, *J. Am. Chem. Soc.* **2006**, *128*, 5992–5993.

[5] M. E. Germain, M. J. Knapp, *J. Am. Chem. Soc.* **2008**, *130*, 5422–5423.

[6] Y.-C. Chou, S.-F. Huang, R. Koner, G.-H. Lee, Y. Wang, S. Mohanta, H.-H. Wei, *Inorg. Chem.* **2004**, *43*, 2759–2761.

[7] Q.-Z. Yang, L.-Z. Wu, H. Zhang, B. Chen, Z.-X. Wu, L.-P. Zhang, C.-H. Tung, *Inorg. Chem.* **2004**, *43*, 5195–5197.

[8] C. S. Consorti, G. Ebeling, F. Rodembusch, V. Stefani, P. R. Livotto, F. Rominger, F. H. Quina, C. Yihwa, J. Dupont, *Inorg. Chem.* **2004**, *43*, 530–536.

[9] H. Jude, J. A. Krause Bauer, W. B. Connick, *Inorg. Chem.* **2004**, *43*, 725–733.

[10] a) M. L. Grachan, M. T. Tidge, E. N. Jacobsen, *Angew. Chem. Int. Ed.* **2008**, *47*, 1469–1472; b) J. Lewiński, P. Horeglad, M. Dranka, I. Justyniak, *Inorg. Chem.* **2004**, *43*, 5789–5791.

[11] A. D. Getty, K. I. Goldberg, *Organometallics* **2001**, *20*, 2545–2551.

[12] a) T. Hara, T. Yamagata, K. Mashima, Y. Kataoka, *Organometallics* **2007**, *26*, 110–118; b) J.-F. Gong, Y.-H. Zhang, M.-P. Song, C. Xu, *Organometallics* **2007**, *26*, 6487–6492; c) Y. Kataoka, K. Shizuma, M. Imanishi, T. Yamagata, K. Tani, *J. Organomet. Chem.* **2004**, *689*, 3–7.

[13] a) F.-B. Han, Y.-L. Zhang, X.-L. Sun, B.-G. Li, Y.-H. Guo, Y. Tang, *Organometallics* **2008**, *27*, 1924–1928; b) J. A. Fuentes, M. L. Clarke, A. M. Z. Slawin, *New J. Chem.* **2008**, *32*, 689–693; c) Z.-X. Wang, L. Wang, *Chem. Commun.* **2007**, 2423–2425; d) A. Del Zotto, W. Baratta, M. Ballico, E. Herdtweek, P. Rigo, *Organometallics* **2007**, *26*, 5636–5642; e) M. L. Clarke, M. B. Díaz-Valenzuela, A. M. Z. Slawin, *Organometallics* **2007**, *26*, 16–19; f) J. Zhang, M. Gandelman, L. J. W. Shimon, D. Milstein, *Dalton Trans.* **2007**, 107–113; g) C. E. Anderson, D. C. Apperley, A. S. Batsanov, P. W. Dyer, J. A. K. Howard, *Dalton Trans.* **2006**, 4134; h) J. Hou, W.-H. Sun, S. Zhang, H. Ma, Y. Deng, X. Lu, *Organometallics* **2006**, *25*, 236–244; i) L. Boubekeur, S. Ulmer, L. Ricard, N. Mézailles, P. Le Floch, *Organometallics* **2006**, *25*, 315–317.

[14] a) S. R. Bayly, A. R. Cowley, J. R. Dilworth, C. V. Ward, *Dalton Trans.* **2008**, 2190–2198; b) P. Pelagatti, A. Bacchi, M. Balordi, S. Bolaño, F. Calbiani, L. Elviri, L. Gonsalvi, C. Pelizzi, M. Peruzzini, D. Rogolino, *Eur. J. Inorg. Chem.* **2006**, 2422–2436; c) O. M. Ní Dhubhghaill, J. Lennon, M. G. B. Drew, *Dalton Trans.* **2005**, 3213–3220; d) S. R. Korupoju, R.-Y. Lai, Y.-H. Liu, S.-M. Peng, S.-T. Liu, *Inorg. Chim. Acta* **2005**, *358*, 3003–3008; e) N. Nimitsiriwat, E. L. Marshall, V. C. Gibson, M. R. J. Elsegood, S. H. Dale, *J. Am. Chem. Soc.* **2004**, *126*, 13598–13599; f) W.-Q. Hu, X.-L. Sun, C. Wang, Y. Gao, Y. Tang, L.-P. Shi, W. Xia, J. Sun, H.-L. Dai, X.-Q. Li, X.-L. Yao, X.-R. Wang, *Organometallics* **2004**, *23*, 1684–1688; g) P.-Y. Shi, Y.-H. Liu, S.-M. Peng, S.-T. Liu, *Organometallics* **2002**, *21*, 3203–3207; h) M. Ahmad, S. D. Perera, B. L. Shaw, M. Thornton-Pett, *J. Chem. Soc., Dalton Trans.* **2002**, 1954–1962; i) P. Pelagatti, A. Bacchi, C. Bobbio, M. Carcelli, M. Costa, C. Pelizzi, C. Vivorio, *Organometallics* **2000**, *19*, 5440–5446; j) P. Bhattacharyya, J. Parr, A. M. Z. Slawin, *J. Chem. Soc., Dalton Trans.* **1998**, 3609–3614; k) E. K. van den Beuken, N. Veldman, W. J. J. Smeets, A. L. Spek, B. L. Feringa, *Organometallics* **1998**, *17*, 636–644.

[15] a) T. Kniess, C. Fernandes, I. Santos, W. Kraus, H. Spies, *Inorg. Chim. Acta* **2003**, *348*, 237–241; b) J. D. G. Correia, A. Domingos, I. Santos, H. Spies, *J. Chem. Soc., Dalton Trans.* **2001**, 2245–2250.

[16] a) C. Gunanathan, D. Milstein, *Angew. Chem. Int. Ed.* **2008**, *47*, 8661–8664; b) L.-C. Liang, P.-S. Chien, P.-Y. Lee, *Organometallics* **2008**, *27*, 3082–3093; c) D. Adhikari, F. Basuli, H. Fan, J. C. Huffman, M. Pink, D. J. Mindiola, *Inorg. Chem.* **2008**, *47*, 4439–4441; d) J. I. van der Vlugt, E. A. Pidko, D. Vogt, M. Lutz, A. L. Spek, A. Meetsma, *Inorg. Chem.* **2008**, *47*, 4442–4444; e) D. Benito-Garagorri, J. Wiedermann, M. Pollak, K. Mereiter, K. Kirchner, *Organometallics* **2007**, *26*, 217–222; f) C. M. Fafard, C.-H. Chen, B. M. Foxman, O. V. Ozerov, *Chem. Commun.* **2007**, 4465–4467; g) A. R. Fout, F. Basuli, H. Fan, J. Tomaszewski, J. C. Huffman, M.-H. Baik, D. J. Mindiola, *Angew. Chem. Int. Ed.* **2006**, *45*, 3291–3295; h) E. Ben-Ari, G. Leitus, L. J. W. Shimon, D. Milstein, *J. Am. Chem. Soc.* **2006**, *128*, 15390–15391; i) D. S. McGuiness, D. B. Brown, R. P. Tooze, F. M. Hess, J. T. Dixon, A. M. Z. Slawin, *Organometallics* **2006**, *25*, 3605–3610; j) D. Benito-Garagorri, E. Becker, J. Wiedermann, W. Lackner, M. Pollak, K. Mereiter, J. Kisala, K. Kirchner, *Organometallics* **2006**, *25*, 1900–1913; k) B. C. Bailey, H. Fan, J. C. Huffman, M.-H. Baik, D. J. Mindiola, *J. Am. Chem. Soc.* **2006**, *128*, 6798–6799; l) S. M. Kloek, D. M. Heinekey, K. I. Goldberg, *Organometallics* **2006**, *25*, 3007–3011; m) M. Porchia, F. Tisato, F. Refosco, C. Bolzati, M. Cavazza-Ceccato, G. Bandoli, A. Dolmella, *Inorg. Chem.* **2005**, *44*, 4766–4776; n) L. Fan, B. M. Foxman, O. V. Ozerov, *Organometallics* **2004**, *23*, 326–328; o) M. S. Rahman, P. D. Prince, J. W. Steed, K. K. Hii, *Organometallics* **2002**, *21*, 4927–4933.

[17] S. E. Durran, M. R. J. Elsegood, M. B. Smith, *New J. Chem.* **2002**, *26*, 1402–1408.

[18] For selected recent examples: a) V. Pandarus, D. Zargarian, *Chem. Commun.* **2007**, 978–980; b) R. B. Bedford, M. Betham, J. P. H. Charmant, M. F. Haddow, A. G. Orpen, L. T. Pilarski, S. J. Coles, M. B. Hursthouse, *Organometallics* **2007**, *26*, 6346–6353; c) L. Ma, R. A. Woloszynek, W. Chen, T. Ren, J. D. Protasiewicz, *Organometallics* **2006**, *25*, 3301–3304.

[19] E. E. Korshin, G. Leitus, L. J. W. Shimon, L. Konstantinovski, D. Milstein, *Inorg. Chem.* **2008**, *47*, 7177–7189.
[20] a) X. Sun, D. W. Johnson, K. N. Raymond, E. H. Wong, *Inorg. Chem.* **2001**, *40*, 4504–4506; b) X. Sun, D. W. Johnson, D. L. Caulder, K. N. Raymond, E. H. Wong, *J. Am. Chem. Soc.* **2001**, *123*, 2752–2763; c) X. Sun, D. W. Johnson, D. L. Caulder, R. E. Powers, K. N. Raymond, E. H. Wong, *Angew. Chem. Int. Ed.* **1999**, *38*, 1303–1307.
[21] M. R. J. Elsegood, M. B. Smith, P. M. Staniland, *Inorg. Chem.* **2006**, *45*, 6761–6770.
[22] I. D. Kostas, B. R. Steele, A. Terzis, S. V. Amosova, A. V. Martynov, N. A. Makhaeva, *Eur. J. Inorg. Chem.* **2006**, 2642–2646.
[23] a) Q. Yao, M. Sheets, *J. Org. Chem.* **2006**, *71*, 5384–5387; b) V. J. Olsson, S. Sebelius, N. Selander, K. J. Szabo, *J. Am. Chem. Soc.* **2006**, *128*, 4588–4589.
[24] J. H. Downing, M. B. Smith, *Phosphorus Ligands* in *Comprehensive Coordination Chemistry II*, Elsevier, Oxford, **2004**, 253–296.
[25] S. E. Durran, M. R. J. Elsegood, S. R. Hammond, M. B. Smith, *Inorg. Chem.* **2007**, *46*, 2755–2766.
[26] M. Oswaw, M. Hoshino, M. Akita, T. Wada, *Inorg. Chem.* **2005**, *44*, 1157–1159.
[27] S. C. F. Kui, J.-S. Huang, R. W.-Y. Sun, N. Zhu, C.-M. Che, *Angew. Chem. Int. Ed.* **2006**, *45*, 4663–4666.
[28] M. B. Smith, S. H. Dale, S. J. Coles, T. Gelbrich, M. B. Hursthouse, M. E. Light, *CrystEngComm* **2006**, *8*, 140–149.
[29] H. Schmidbaur, A. Schier, *Chem. Soc. Rev.* **2008**, *37*, 1931–1951.
[30] S. Chikkali, S. Magens, D. Gudat, M. Nieger, I. Hartenbach, T. Schleid, *Eur. J. Inorg. Chem.* **2008**, 2207–2213.
[31] a) M. B. Smith, A. M. Z. Slawin, *New J. Chem.* **2000**, *24*, 65–67; b) A. M. Z. Slawin, M. B. Smith, *New J. Chem.* **1999**, *23*, 777–783.
[32] Y. Yamamoto, X.-H. Han, S. Nishimura, K.-i. Sugawara, N. Nezu, T. Tanase, *Organometallics* **2001**, *20*, 266–272.
[33] R. Uson, A. Laguna, M. Laguna, *Inorg. Synth.* **1989**, *26*, 85–91.
[34] a) D. Drew, J. R. Doyle, *Inorg. Synth.* **1972**, *13*, 47–55; b) J. X. McDermott, J. F. White, G. M. Whitesides, *J. Am. Chem. Soc.* **1976**, *98*, 6521–6528.
[35] M. A. Bennett, A. K. Smith, *J. Chem. Soc., Dalton Trans.* **1974**, 233–241.
[36] C. White, A. Yates, P. M. Maitlis, *Inorg. Synth.* **1992**, *29*, 228–234.
[37] a) A. C. Cope, E. C. Friedrich, *J. Am. Chem. Soc.* **1968**, *90*, 909–913; b) A. C. Cope, R. W. Siekman, *J. Am. Chem. Soc.* **1965**, *87*, 3272–3273.
[38] *SMART* and *SAINT* software for CCD diffractometers, Bruker AXS Inc., Madison, WI, **2001**.
[39] *COLLECT*: Data Collection Software, R. Hooft, Nonius B. V., **1998**.
[40] *DENZO*, Z. Otwinowski, W. Minor, in: C. W. Carter Jr., R. M. Sweet (Eds.), *Methods in Enzymology, Macromolecular Crystallography*, part A, vol. 276, Academic Press, **1997**, 307–326.
[41] a) G. M. Sheldrick, *SHELXTL* user manual, version 6.10, Bruker ACS Inc., Madison, WI, **2000**; b) G. M. Sheldrick, *Acta Crystallogr., Sect. A* **2008**, *64*, 112.
[42] A. L. Spek, *Acta Crystallogr., Sect. A* **1990**, *46*, C34.

Received: November 12, 2008
Published Online: February 6, 2009

